Pharmacological Reports 71 (2019) 591–602

Contents lists available at ScienceDirect

Pharmacological Reports

journal homepage: www.elsevier.com/locate/pharep

Original article

# Doxorubicin-induced testicular damage is related to PARP-1 signaling molecules in mice

Nazli Ece Gungor-Ordueri[a], Nilay Kuscu[b], Arda Tasatargil[c], Durmus Burgucu[d], Meric Karacan[e], Ciler Celik-Ozenci[b,*]

[a] Department of Histology and Embryology, Medical Faculty of Biruni University, Campus, Istanbul, Turkey
[b] Department of Histology and Embryology, Medical Faculty of Akdeniz University, Campus, Antalya, Turkey
[c] Department of Pharmacology, Medical Faculty of Akdeniz University, Campus, Antalya, Turkey
[d] Antalya Technopark Babylife Cord Blood Bank and Stem Cell Research Center, Antalya, Turkey
[e] Department of Obstetrics and Gynecology, Medical Faculty of Yeni Yuzyıl University, Istanbul, Turkey

ARTICLE INFO

*Article history:*
Received 18 December 2017
Received in revised form 21 February 2019
Accepted 26 February 2019
Available online 27 February 2019

*Keywords:*
Doxorubicin
PARP-1
PJ34
Apoptosis
Testicular damage
Male infertility

ABSTRACT

*Background:* Doxorubicin (DOX), is a chemotherapeutic agent, which evokes oxidative stress and cell apoptosis in testicular tissue. It is known that the activation of the nuclear enzyme poly (ADP-ribose) polymerase (PARP), leading to apoptosis induced by DOX. The aim of the present study is to investigate whether PARP pathway has a role in DOX-induced testicular damage and infertility utilizing pharmacological PARP-1 inhibitor, PJ34, and PARP-1 knockout mice model.

*Methods:* Firstly, we assessed the activation of PARP pathway after DOX-induction at various hours by immunohistochemistry and western blot analysis. Secondly, we evaluated the role of PARP pathway in DOX-induced testicular damage, sperm motility, and fertility with pharmacological inhibition of PARP by using PJ34. Finally, we aimed to correlate a functional relationship between PARP-1 and DOX using PARP-1 knockout mice in DOX-induced testicular damage. Doxorubicin levels in plasma and testis tissue were also assessed.

*Results:* In DOX-induced group; PARP-1, PAR and apoptotic pathway protein expressions, increased significantly. In DOX + PJ34 group; PAR, cytochrome c, and AIF levels decreased significantly. Testicular weights, sperm motility, and mean the number of pups per litter decreased in DOX-induced group after 28 days, however they were similar to the control group in DOX-PJ34 group. In PARP-1 KO group, seminiferous tubule morphology was impaired significantly after 28 days of DOX-administration.

*Conclusions:* Our study indicates that DOX-induced testicular damage may be related to over-activation of PARP-1. PJ34 application was effective in preventing severe testicular damage caused by DOX-injection and may be considered for fertility protection against DOX-induced testicular damage.



## Introduction

Advances in chemotherapy in the treatment of cancers such as Hodgkin lymphoma, non-Hodgkin lymphoma, leukemia and testicular cancer increased the life expectancy significantly. While some cancers are indeed curable, patients may suffer from long-lasting side effects, e.g. gonadal dysfunction, due to the toxicity of the treatment received. Although some patients may eventually regain fertility spontaneously after years, it is crucial to prevent infertility related to gonadal dysfunction as a result of chemotherapy. It is clearly known that the testicular damage can be induced by chemotherapy, however, the mechanism, which disrupts spermatogenesis is not fully elucidated [1,2]. DOX is a widely used anthracycline antibiotic that acts by intercalating DNA to suppress proliferation and stimulate apoptosis, being effective in a large variety of cancers [3]. DOX may have dose-dependent toxic side effects on bone marrow, heart, and kidney as well as testes, causing germ cell loss [4–6].

Poly (ADP-ribose) polymerases (PARPs), which is also called poly (ADP-ribose) synthetase (PARS), is a group of enzymes found in eukaryotic cells and involved in many cellular functions [7,8]. Single-strand DNA breaks induced by reactive oxygen and nitrogen species activate PARP, which then attaches to the region of damage and catalyzes the synthesis of poly (ADP-ribose) (PAR), serving as a

* Corresponding author.
*E-mail address:* cilerozenci@akdeniz.edu.tr (C. Celik-Ozenci).

http://dx.doi.org/10.1016/j.pharep.2019.02.018

signal for repair enzymes to access to damaged DNA [9]. After DNA damage has been repaired, PAR polymers are degraded by poly (ADP-ribose) glycohydrolase (PARG), which catalyzes the hydrolysis of PAR [10]. During this process, PARP produces ADP-ribose polymers, which initiates an energy-consuming cycle by transferring ADP ribose units from nicotinamide (NAD+) to nuclear proteins, resulting in the rapid depletion of the intracellular NAD and ATP pools [8].

Under physiological conditions, main function of PARP is to detect and repair DNA damage, playing a protective role [11]. However, in the presence of excessive DNA damage PARP becomes over-activated and cause tissue damage and cell death [12–16]. Inhibition of PARP-1 overactivity utilizing PARP inhibitors has been commonly considered in the literature as a strategy to prevent tissue damage [17,18].

Until recently, 18 members of the PARP family have been identified. Of these, PARP-1 and PARP-2 have overlapping functions during the repair of DNA breaks by base excision repair/single-strand break repair pathways [19].

The aim of the present study is to investigate whether PARP pathway has a role in DOX-induced testicular damage and infertility utilizing pharmacological PARP-1 inhibitor, PJ34 and PARP-1 knockout mice model.

## Materials and methods

### *Experimental animals*

Six-weeks-old C57BL male wild-type mice were obtained from Akdeniz University Animal Research Unit and mice were housed under temperature and light-controlled conditions (22 °C ± 1 °C, 12 h light/12 h dark cycle) with ad libitum access to food. Four main groups were established with wild-type mice: Control, DOX-induced, PJ34, and DOX + PJ34 [20]. In the other setting, 25–30 g PARP-1 non-mutant (PARP-1 NM, 129S-tm1Zqw/J) and PARP-1 knockout (PARP-1 KO) male mice (129S-Parp1tm1Zqw/J) obtained from Jackson Laboratory (Bar Harbor, ME, USA) were used. Experimental protocol was approved by the animal care and usage committee of Akdeniz University and was in accordance with the Institutional Animal Care and Use Committee (IACUC) guide.

### *Study design*

Various experiments have been designed to evaluate the role of PARP-1 pathway in testicular damage and fertility after DOX-induction. In experiment 1a, we performed a single DOX injection (*intraperitoneally (ip)* 9 mg/kg) and removed the testes of wild-type mice after 0 (control), 1, 2, 4, 6, and 8 h. In experiment 1b, we performed a single DOX injection (9 mg/kg) together with PJ34 treatment and removed the testes of wild-type mice after 4 h (since there was a significant increase in PARP-1 expression after 4 h). In experiment 2, we performed consecutive DOX injections (3 mg/kg every following 2 days- an accumulated dose of 9 mg/kg) together with PJ34 injection (20 mg/kg *ip* was started 1 h before the first DOX injection and continued (3 × 10 mg/kg *ip*/day) and removed the testes of wild-type mice after 7 and 28 days. In experiment 3, DOX injection together with PJ34 has been performed (as explained in experiment 2) to PARP-1 KO mice and its control PARP-1 NM mice, and testes were removed after 7 and 28 days.

To test our hypothesis, doxorubicin levels in plasma and testis tissue, PARP activity, caspase-dependent and caspase-independent apoptosis signaling proteins were assessed. Testicular and body weights, testis histopathology, sperm motility, and number of pups per litter were also evaluated.

*Experiment 1a: evaluation of PARP activation, apoptosis pathways at various hours after single dose DOX-injection*

Six groups (n = 6 mice per group) were established after DOX-induction (a single 9 mg/kg dose injection) 0 h served as a control, 1 h, 2 h, 4 h, 6 h, and 8 h. DOX levels were measured in plasma and testicular tissue to confirm its presence after 2 h, 4 h, and 7 days utilizing reversed-phase-liquid chromatography (RP-HPLC) method. Expression of PARP-1 and PAR was evaluated by immunohistochemistry. Moreover, full length PARP-1, PAR, cleaved PARP-1, cleaved caspase-3, p53, p21, cytochrome c, and AIF expressions were determined by western blot analysis. Beta-actin and/or GAPDH served as internal control to confirm equal loading of proteins for western blot analysis.

*Experiment 1b: evaluation of PAR, AIF, and cytochrome c expression after 4 h following DOX-injection together with PJ34 treatment*

Four groups (n = 6 mice per group) were established: Control group (C), DOX injection group (DOX), DOX injection with PJ34 treatment (DOX + PJ34) and PJ34 treatment group (PJ34). A single dose of 9 mg/kg *ip.* DOX injection together with a single dose of 20 mg/kg *ip.* PJ34 injection was performed and testes were collected after 4 h. Expression of PAR, cytochrome c, and AIF was evaluated by western blot analysis.

*Experiment 2: evaluation of testicular damage, sperm motility, and fertility after 7 and 28 days following DOX-injection together with PJ34 treatment*

Four groups (n = 6 mice per group) were established: Control group (C), DOX injection group (DOX), DOX injection with PJ34 treatment (DOX + PJ34) and PJ34 treatment group (PJ34). Consecutive DOX injections (3 mg/kg every following 2 days- an accumulated dose of 9 mg/kg) together with PJ34 injection (20 mg/kg *ip* was started 1 h before the first DOX injection and continued (3 × 10 mg/kg *ip*/day) and testes were removed from wild-type mice after 7 and 28 days. Doxorubicin dose utilized in our study was similar with the previous studies [1,21]. It is known that the pharmacokinetics of DOX is characterized by an initial rapid tissue distribution phase (half-life [t1/2], 10 min), followed by a prolonged elimination phase [t1/2, 30 h) [22–24]. Therefore, we performed PJ34 treatment (3 × 10 mg/kg *ip*/day) for five days after the last DOX administration. Dose of PJ34 was adapted from previous *in vivo* studies demonstrating the efficacy and potency of the drug to inhibit PARP activity without any resultant toxicity. Treatment with the PARP inhibitor PJ34 (20 mg/kg *ip* was started 1 h before the first DOX injection and continued (3 × 10 mg/kg *ip*/day) five days after the last DOX administration. A similar dosing regimen with PJ34 has previously been shown to be sufficient to block vascular PARP activation in rats and mice [7,25,26]. This treatment regimen has also previously been shown to inhibit PARP activation in various tissues in rodent experiments *in vivo* [27–29]. We aimed to detect an early impact of DOX on day 7 and also on day 28, which corresponds to the end of the first wave of the spermatogenetic cycle in mice. Testicular and body weights, testis histopathology (utilizing Johnsen Score), sperm motility, and number of pups per litter were evaluated.

*Experiment 3: evaluation of testicular damage after 7 and 28 days following DOX-injection in PARP-1 knockout mice*

Six groups (n = 8 mice per group) were established: PARP-1 non-mutant (PARP-1-NM) control group, PARP-1 knockout (PARP-1 KO) group, ip DOX-injected (consecutive DOX injections 3 mg/kg every following 2 days- an accumulated dose of 9 mg/kg) PARP-1-NM and sampling were done after 7 days (DOX-NM-7) group, *ip* DOX-injected (consecutive DOX injections 3 mg/kg every following 2 days- an accumulated dose of 9 mg/kg) PARP-1-NM and sampling were done after 28 days (DOX-NM-28) group, *ip* DOX-injected

(consecutive DOX injections 3 mg/kg every following 2 days- an accumulated dose of 9 mg/kg) PARP-1-KO and sampling were done after 7 days (DOX-KO-7) group, and *ip* DOX-injected (consecutive DOX injections 3 mg/kg every following 2 days- an accumulated dose of 9 mg/kg) PARP-1-KO and sampling were done after 28 days (DOX-KO-28) group. Testicular and body weights and testis histopathology (utilizing Johnsen Score) were evaluated.

*Reversed-phase - liquid chromatography (RP-HPLC) method*

DOX levels of blood and testis were measured by RP-HPLC system (Shimadzu, Columbia, MD, USA) which consisting of a LC10AD VP pump and a Shimadzu RF-10AXL fluorescence detector (excitation wavelength 365 NM; emission wavelength 470 NM). Separation was carried out on a Phenomenex Luna 3 μm C18 (2) column (150 × 4.6 mm i.d.; 3 μm particle size) with a Phenomenex pre-column C18 (ODS, Octadecyl; 4.0 × 3.0 mm i.d.; 5 μm particle size, Torrance, CA, USA). Mobile phase having methanol-ACN-water (95 + 3 + 2, v/v/v) was pumped at 1.1 ml/min, and 20 μl of sample was injected into the HPLC system.

*Plasma sample preparation for chromatography*

One milliliter of acetonitrile (ACN): water (4 + 1, v/v) was added to each plasma sample (1 ml) and they were vortexed for 5 min. The samples were centrifuged at room temperature for 5 min at 2000 × *g*. After centrifugation, the supernatant was taken and transferred to a reservoir connected to a Bakerbond Octyl (C8) cartridge. The cartridge was previously activated with 5 ml of methanol and conditioned with 5 ml of water. After applying the sample extract, the cartridge was washed with 2 ml of water followed by 1 ml water: methanol (3 + 1, v/v). The analyte was eluted with 1.2 ml of methanol, collected in a polypropylene test tube and evaporated to dryness under nitrogen at 60 °C. Plasma were then derivated with 100 μl of NMI in ACN (1 + 1, v/v) and 150 μl of TFAA in ACN (1 + 1, v/v). A 20-μl aliquot of the sample was then injected into the HPLC system. For quantification purposes, calibration curves for DOX were prepared. The addition of 20 μl of the standard working solutions resulted in calibration curves with DOX concentrations of 1–100 ng/ml plasma. The curves were linear over this range (r = 0.998). The detection limit (LOD) and the limit of quantitation (LOQ) were defined as three and ten standard deviations plus mean blank value, respectively. LOD and LOQ values were calculated as 0.05 and 0.12 ng/ml for DOX, respectively.

*Testis tissue sample preparation procedure for chromatography*

Five ml of ACN was added to 1 mg weighted, homogenized testis tissue and vortexed for 5 min. Samples were placed in ultrasonic shaker for 10 min. After centrifugation (10 min, 2600 rpm, room temperature), a 5 ml portion of extract was taken and diluted to 10 ml with doubly distilled water followed by addition of 50 ml of TEA. The sample was then transferred to a reservoir connected to a Bakerbond Octyl (C8) cartridge. The cartridge was previously activated with 5 ml of ACN and conditioned with 5 ml of ACN–water–TEA (50 + 50 + 0.1, v/v/v). After applying the sample extract, the analyte was eluted with 5 ml of ACN, collected in a polypropylene test tube and evaporated to dryness under nitrogen at 60 °C. Tissue samples were then derivatized with 100 ml of NMI in ACN (1 + 1, v/v) and 150 ml of TFAA in ACN (1 + 1, v/v). An 20 ml aliquot of the sample was then injected into the HPLC system.

*Sperm motility analysis*

The epididymis from each group was removed and washed three times with human tubular fluid (HTF), which has been developed for *in vitro* procedures that require sperm washing (Irvine Scientific, USA, cat #9983) to remove surface blood [30]. It was then placed in a petri dish with 5 ml of pre-heated at 37 °C HTF medium. The tissue was minced with scalpels and placed in a 37 °C incubator for 10 min, prior to assessing sperm movement. The suspension was stirred, one drop placed on a Makler chamber, and sperm counts and percentage of motile cells were calculated. [31]. At least five widely spaced fields were examined to provide an estimated percentage of motile sperm.

*Western blot analysis*

Protein concentration determination and western blotting were applied as described before [32]. Prior to electrophoresis, samples were boiled for 5 min at 95 °C. Samples were subjected to SDS-polyacrylamide gel electrophoresis and then were transferred onto PVDF membranes (162-0177; Bio-Rad, Hercules, CA, USA) in a buffer containing 0.2 M glycine, 25 mM Tris and 20% methanol overnight. Blotting membranes were incubated for 2 h at room temperature with rabbit polyclonal anti-PARP-1 (1:200, Ab6079; Abcam, Cambridge, UK), mouse monoclonal anti-PAR (1:500, ALX-804-220-R100; Alexis, BD, Franklin Lakes, NJ, USA), rabbit polyclonal anti-cleaved PARP-1 (1:100, 9548S Cell Signaling; Danvers, MA, USA), rabbit polyclonal cleaved caspase-3 (1:200, 9979; Cell Signaling Danvers, MA, USA), rabbit polyclonal anti-p53 (1:250, sc-6243; Santa Cruz, TX, USA), rabbit polyclonal anti-p21 (1:250, sc-22305, Santa Cruz, TX, USA), rabbit polyclonal anti-cytochrome c (1:50, 4272S; Cell Signaling Danvers, MA, USA) and rabbit polyclonal anti-AIF (apoptosis-inducing factor) (1:1000 4642S; Cell Signaling, Danvers, MA, USA) antibodies. After washing with Tris-PBS buffer, membranes were further incubated with the secondary anti-rabbit or mouse (dilution: 1:5000, PI-1000; Vector Lab,) horseradish peroxidase-conjugated antibodies for 1 h at room temperature. Labeling was visualized using the chemiluminescence based Super Signal CL-HRP Substrate System (Pierce, Rockford, IL, USA) and the membranes were exposed to Hyperfilm (GE Healthcare, Amersham). As an internal control, Beta-actin antibody at the dilution of 1:3000 (Ab8229; Abcam) or glyceraldehyde-3-phosphate dehydrogenase (GAPDH) antibody at 1:1000 (2118S, Cell Signaling) were used to confirm equal loading of the proteins. Protein bands were measured by Image J Software (LOCI, University of Wisconsin) and reflected to the histogram. In some experiments, due to distant loading order in the same gel, we put some of western blot band results together by cutting and pasting them to express the levels of the proteins in the following order. These have been indicated in western blot figures by vertical lines.

*Immunohistochemistry*

Testicular tissues of mice were fixed in Bouin's fixative (75% picric acid, 5% glacial acetic acid, and 25% formaldehyde) for 4 h, dehydrated in ethanol, embedded in paraffin. Testes tissue sections were deparaffinized in xylene and then rehydrated through a decreasing gradient of ethanol for immunohistochemical labeling. Antigen retrieval was performed in citric acid (pH 3.5; ≥90 °C maintained for 10 min). Rabbit polyclonal anti-PARP-1 (Ab6079; Abcam, Cambridge, UK), mouse monoclonal anti-PAR (ALX-804-220-R100; Alexis, BD, Franklin Lakes, NJ, USA), primary antibodies, applied at 1.0 and 2.0 mg/ml in 0.1% bovine serum albumin (BSA)/Tris-buffered saline (TBS) for overnight incubation, respectively. Negative controls were performed by omitting primary antibody, but applying 0.1% BSA/TBS on sections. Subsequent steps were performed at room temperature with TBS washes between incubations. Primary antibody bindings were detected using a

biotinylated anti-rabbit and anti-mouse secondary antibody (Vector Laboratories, Burlingame, CA, USA; 1:500 dilution, 1 h) then with the Vectastain Elite ABC kit according to the manufacturer's instructions (Vector Laboratories). Antibody interactions were detected as a brown precipitate following development with 3,3-diaminobenzidine tetrahydrochloride (DAB), with Harris Hematoxylin used as a counterstain. Sections were mounted under glass coverslips in Entellan solution (Merck Millipore, Darmstadt, Germany). At least three independent samples were examined for each antibody. Photomicrographs were taken using an Axioplan microscope (Zeiss, Oberkochen, Germany). Expression levels of proteins were evaluated from at least three different fields of sections per group and defined as low (+), moderate (++), and high (+++) expression semi-quantitatively.

*Histological evaluation*

Testicular tissue sections were stained with hematoxylin and eosin. Tubule degeneration was evaluated in each group by Johnsen score [33]. Sections were examined in a random order under a standard light microscope at 10x magnification by a blinded histologist; unaware of which group each mouse belonged to. Approximately 80 randomly selected seminiferous tubules per mice were evaluated. Thus, a total of approximately 640 seminiferous tubules were scored for each group. The Johnsen scoring system is principally based on the progressive degeneration of germinal epithelium and a successive loss of the most mature cell types during testicular damage. It applies a grade from 1 to 10 to each tubule cross section; 10 being complete spermatogenesis and perfect tubules whereas 1 being no germ cells and no Sertoli cells present.

*Mating evaluation*

Mating was confirmed by the presence of a vaginal plug and females were housed to monitor weight gains indicating pregnancy for 15 days. If no weight gain occurred after 15 days, the animals were re-mated at proestrus. If no vaginal plug was observed, females were left in continuous pairings with males for 4 days and then weighted for 15–21 days. Mating rates and number of pups per litters (live births) were recorded.

*Statistical analysis*

Data are presented as the mean ± SEM and were analyzed using Sigmaplot Software, version 13. Significant findings were further compared by One-way analysis of variance with Tukey *post-hoc* test. Levels of significance were set at $p < 0.05$.

## Results

*Doxorubicin levels in plasma and the testis*

Doxorubicin levels were assessed in plasma and the testis in each group. DOX retention time was ~3.05 min in plasma. Doxorubicin levels were 91.8 ± 12.2 ng/ml, 112.9 ± 18.5 ng/ml, and 1.3 ± 0.6 ng/ml at 2 h, 4 h, and 7 days after DOX-administration, respectively (Fig. 1A). These results indicated that the significant increase in DOX levels at 2 h and 4 h decreased at 7 days ($p < 0.05$) although there was still some amount of DOX in the plasma.

In the testis, DOX retention time was ~3.1 min. The DOX levels were 2.9 ± 0.7 ng/mg and 0.02 ± 0.02 ng/mg at 4 h and 7 days after DOX-administration, respectively (Fig. 1B). These results indicated that the significant increase in DOX levels at 4 h decreased at 7 days ($p < 0.05$) although there was still some amount of DOX in the testis. DOX levels of testicular tissue at 2 h after DOX-administration was not assessed because of its proximity with 4 h analysis.

*Expression levels of PARP-1 and PAR at various hours after single dose DOX-injection*

PARP-1 expression was detected essentially in the nuclei of spermatogonia (0 h) and its expression increased at 2 h and 4 h after DOX-injection. In addition to its spermatogonial expression, nuclear PARP-1 expression increased gradually in spermatocytes and round spermatids starting from 2 h to 8 h after DOX-injection (Fig. 2A). PARP-1 expression levels evaluated semi-quantitatively were presented in (Fig. 2B). PAR expression was present in nuclei of spermatogonia at 0, 2, 4, 6, and 8 h and its expression increased at 4 h and 8 h after DOX-injection (Fig. 2C). PAR expression levels evaluated semi-quantitatively were presented in (Fig. 2D). Altogether, expression levels of both PARP-1 and PAR increased at 4 h after DOX-injection.

*Expression levels of full length PARP-1, PAR, cleaved PARP-1, cleaved caspase-3, p53, p21, cytochrome c, and AIF at various hours after single dose DOX-injection*

In testes, PARP activation was confirmed by detecting increased expression of full-length PARP-1, PAR and cleaved PARP-1 proteins at 2 h and 4 h after DOX-injection (Fig. 3A). Full-length PARP-1 expression increased at 2 h and 4 h after DOX-injection but its increase was not statistically significant (Fig. 3B). PAR expression increased significantly at 2 h and 4 h (Fig. 3B). Cleaved caspase-3 expression increased significantly at 2 h and 4 h after DOX-injection (Fig. 3A and B). Expression of caspase-dependent

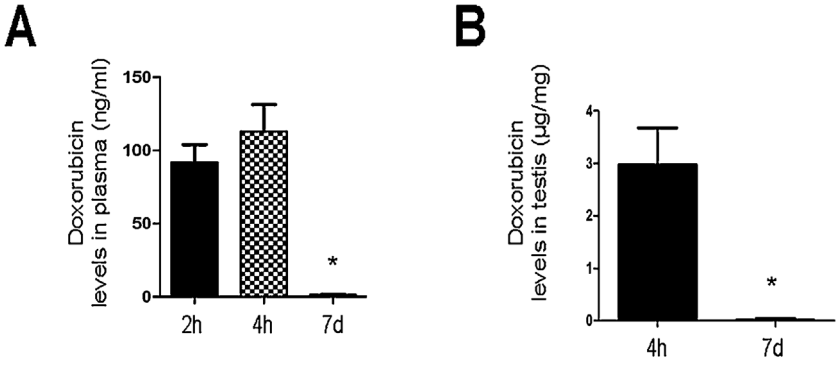


**Fig. 1.** Doxorubicin (DOX) levels in plasma (A) and testis (B) were measured using RP-HPLC method. Doxorubicin levels in plasma (ng/mL) and testis (µg/mg) were indicated by histogram at 2 hours, 4 hours, and 7 days after DOX-administration. Doxorubicin levels increased significantly both in plasma and testis at 2 hours and 4 hours (*$p$<0.05).

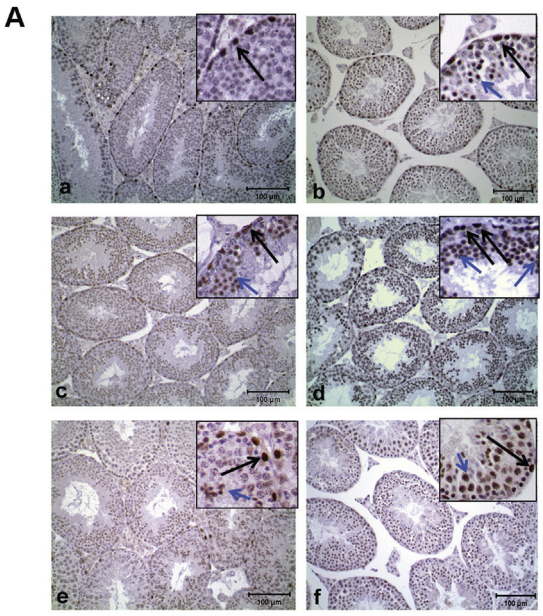


B

| | Protein expression levels | |
|---|---|---|
| PARP-1 | 0h | + |
| | 1h | + |
| | 2h | ++ |
| | 4h | +++ |
| | 6h | +++ |
| | 8h | ++ |

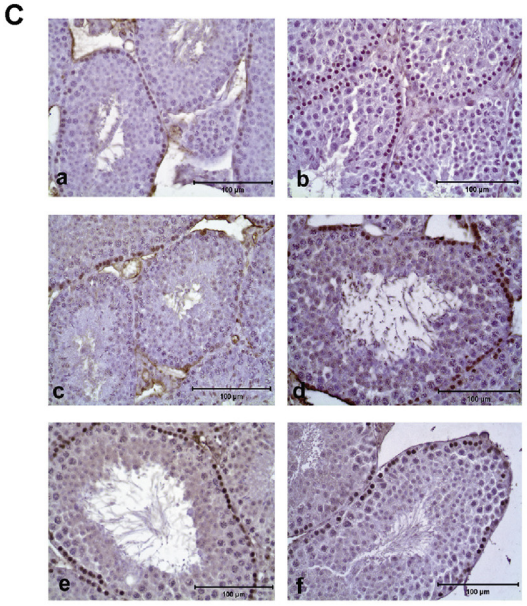


D

| | Protein expression levels | |
|---|---|---|
| PAR | 0h | + |
| | 1h | + |
| | 2h | + |
| | 4h | ++ |
| | 6h | ++ |
| | 8h | + |

**Fig. 2.** Immunohistochemical analysis of PARP-1 (A, B) and PAR (C, D) at various hours after DOX-administration. (a) 0 h (0h), (b) 1 h (1h), (c) 2 h (2h), (d) 4 h, (e) 6 h, and (f) 8 hours (8h). (A) Increased PARP-1 expression in spermatogonia (black arrows) and spermatocytes (blue arrows) after 2h can be seen in detail in highlighted boxes with higher magnifications of corresponding images. (B) Increased PAR expression in spermatogonia after 2h could be seen. Protein expression levels evaluated semi-quantitatively have been presented in B and D. Scale bars: 100 μ.

apoptotic pathway proteins, p53 and p21, increased significantly at 2 h and 4 h after DOX-injection (Fig. 3A and B). Expression of caspase-independent apoptotic pathway proteins, AIF and cytochrome c, increased significantly at 2 h and 4 h after DOX-injection (Fig. 3A and B).

*Evaluation of PAR, AIF, and cytochrome c expression after 4 h following DOX-injection together with PJ34 treatment*

PAR expression in DOX group was significantly higher when compared to control, DOX + PJ34, and PJ34 groups indicating that PARP-1 inhibition was successful by PJ34 (Fig. 4A and B). Cytochrome c and AIF expression increased significantly in DOX and DOX + PJ34 groups when compared to control and PJ34 groups. Although their expression levels were lower in the DOX + PJ34 group than in DOX group, it did not reach to statistically significant level (Fig. 4C–E).

*Evaluation of testicular damage after 7 and 28 days following DOX-injection together with PJ34 treatment and in PARP-1 knockout mice*

Control, DOX-7, DOX + PJ34-7, and PJ34-7 groups had normal spermatogenesis with similar Johnsen scores (Fig. 5A and C) whereas in DOX-28 group there was a significant testicular damage with decreased Johnsen score (Fig. 5B and C). This testicular damage caused by DOX was prevented to some extent in DOX + PJ34-28 group (Fig. 5B and C) indicated by a better Johnsen score.

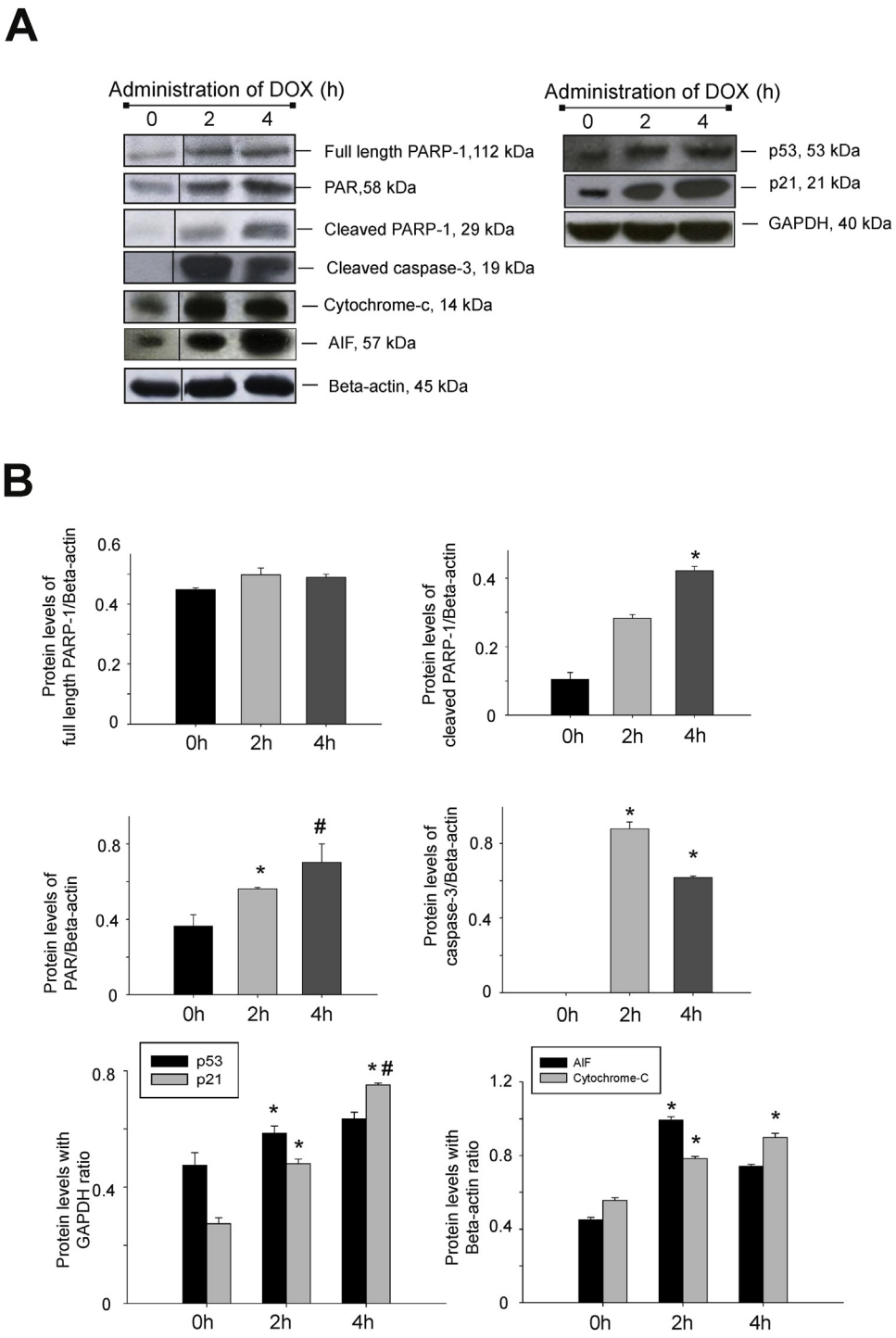


**Fig. 3.** Western blot analysis of full length PARP-1, PAR, cleaved PARP-1, cleaved caspase-3, p53, p21, cytochrome c, and AIF at various hours after single dose DOX-injection (A) Testis lysates were used for western blotting to assess the steady-state protein levels at 0 h (0), 2 h (2) and 4 h (4). (B) Analysis of western blot results were presented where each bar represents mean ± SEM of three samples per group (n=6 mice were included in each group). β-Actin and GAPDH was loaded to the gels as internal standards to confirm the equal loading of the proteins. $p<0.05$ for * and # in different pairwise comparisons.

Moreover, we analyzed the testicular damage in DOX-injected PARP-1-NM and PARP-1 KO mice after 7 and 28 days. In PARP-1 NM testicular damage was present after 28 days of DOX-injection with a significant decrease in Johnsen score (Fig. 5D and E) whereas in PARP-1 KO mice DOX-injection caused significant testicular damage with decreased Johnsen scores both at 7 and 28 days indicating that if there is no PARP-1, testicular damage due to DOX is worsened (Fig. 5D and F).

*Evaluation of fertility after DOX-injection together with PJ34 treatment*

We showed the maintenance of spermatogenesis by mating male mice in experiment 2 with mature virgin female mice to test their fertilization potential. Mating rates and live birth rates were evaluated. In control, DOX, DOX + PJ34 and PJ34 groups, mating rates was 7/8 (87.5%), 1/8 (12.5%), 3/8 (37.5%), and 7/8 (87.5%),

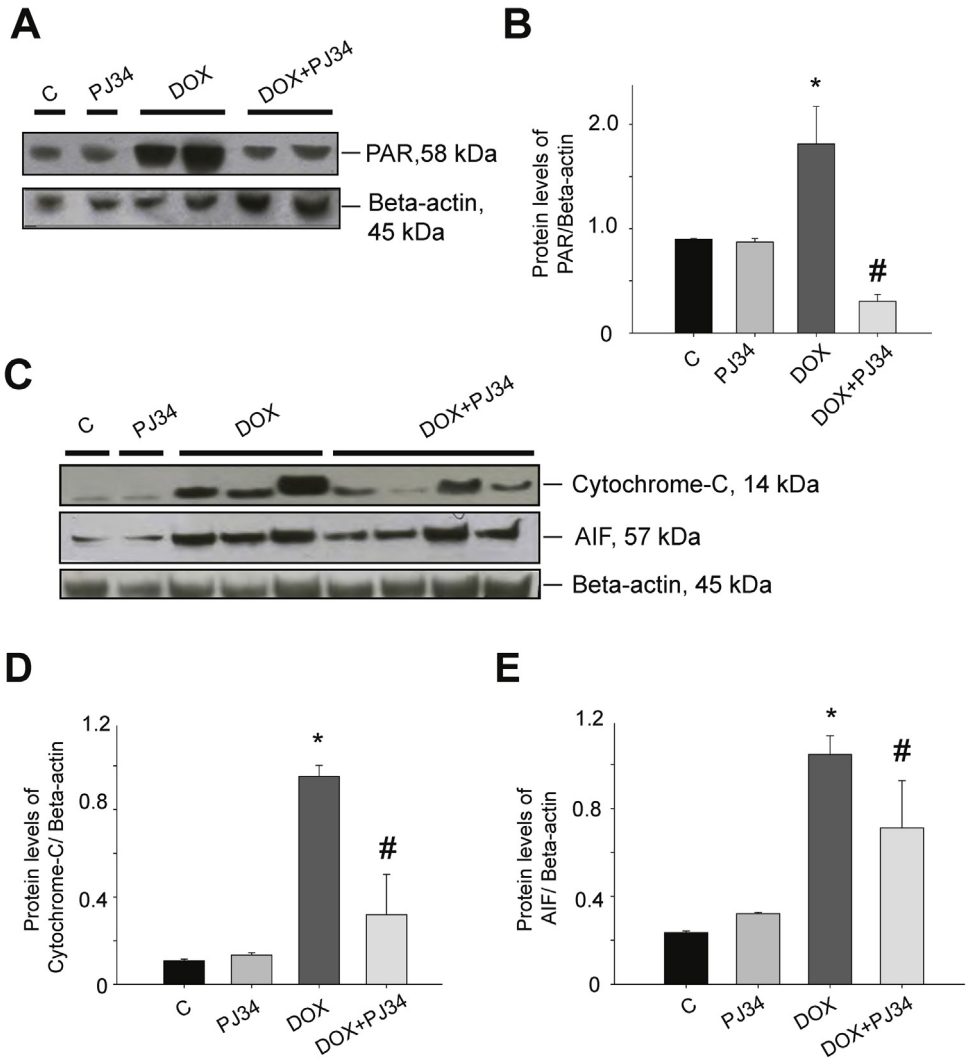


**Fig. 4.** Western blot analysis of PAR, AIF, and cytochrome c expression after 4 h following DOX-injection together with PJ34 treatment. (A, B) PAR expression in DOX group was significantly higher when compared to control, DOX+PJ34, and PJ34 groups indicating that PARP-1 inhibition was successful by PJ34. (C-E) Cytochrome c and AIF expression increased significantly in DOX and DOX+PJ34 groups when compared to control and PJ34 groups. Although their expression levels were lower in the DOX+PJ34 group than in DOX group, it was not significant. (B, D, E) Analysis of western blot results was presented where each bar represents mean ± SEM of three samples per group (n=6 mice were included in each group). β-Actin was loaded to the gels as an internal standard to confirm the equal loading of the proteins. $p<0.05$ for * and # in different pairwise comparisons.

respectively (Table 1). Mean number of pups per litter was significantly lower in DOX group ($4 \pm 0$) when compared to control, DOX + PJ34, and PJ-4 groups being $7.1 \pm 0.8$, $7.3 \pm 0.9$, and $7.5 \pm 0.9$, respectively (Table 1).

*Evaluation of sperm motility after DOX-injection together with PJ34 treatment*

Sperm motility decreased at 7 day after DOX-injection but this decrease was not significant (Fig. 6A) whereas sperm motility decreased significantly at 28 day after DOX-injection (Fig. 6B). Administration of PJ34 together with DOX-injection significantly prevented the decrease in sperm motility (Fig. 6B).

*Evaluation of testis and body weights after DOX-injection together with PJ34 treatment and in PARP-1 knockout mice*

In experiment 2, weights of both testes, which were normalized with body weight, were assessed in control, DOX, DOX + PJ34, and PJ34 groups. Testis weights decreased significantly in DOX group both at day 7 and day 28 after DOX-injection (Fig. 7A and B) whereas PJ34 administration prevented this decrease both at day 7 and day 28 after DOX-injection (Fig. 7A and B). In PARP-1 knockout mice, testis weights decreased significantly in DOX-7-PARP-1-KO, DOX-28-PARP-1-NM, and DOX-28-PARP-1-KO groups (Fig. 7C) confirming our previous result that if there is no PARP-1, testicular damage due to DOX is worsened.

## Discussion

Tissue damage and apoptosis induced by DOX in testes is an important issue and limited data is present in the literature. Results of our study indicate that DOX-induced testicular damage, germ cell apoptosis, and infertility may be related to over-activation of PARP-1. PJ34, a potent PARP inhibitor, application was effective in preventing severe testicular damage caused by DOX-injection and may be considered for fertility protection against DOX-induced testicular damage.

Under physiological conditions or limited DNA damage, the primary function of PARP-1 is to detect and repair DNA damage, thus PARP plays a protective role in these conditions [34,35]. On the other hand, over-activation of PARP represents an important

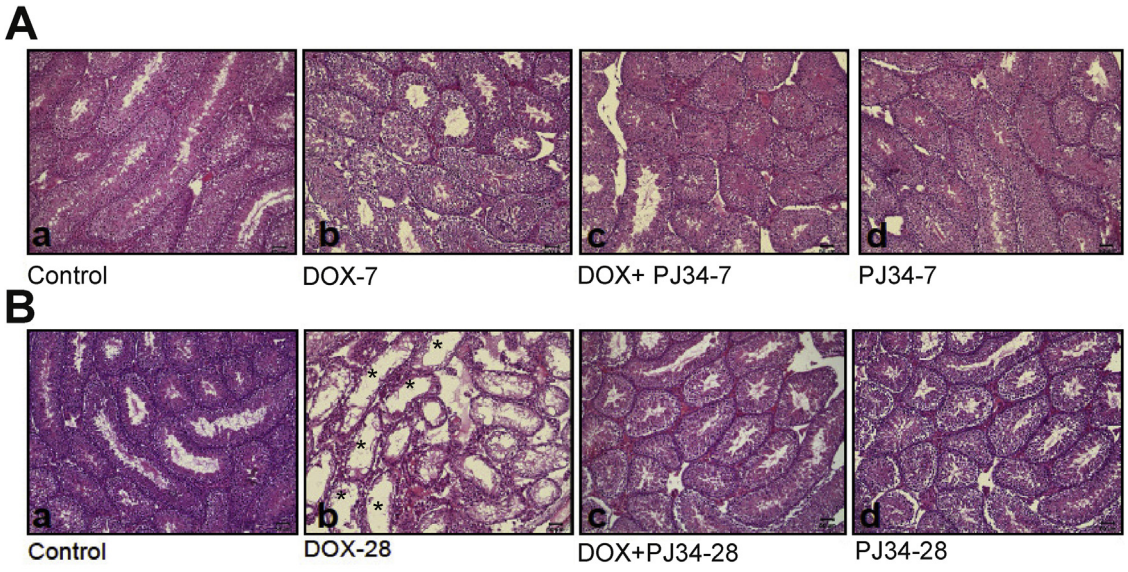


C

**Johnsen Score Analysis (*$p < 0.05$)**

| | |
|---|---|
| Control | 9.25 ± 0.5 |
| DOX-7 | 7.25 ± 0.95 |
| DOX+ PJ34-7 | 8 ± 0.82 |
| PJ34-7 | 8.5 ± 0.58 |
| DOX-28 | 4.5 ± 0.58* |
| DOX+ PJ34-28 | 7.25 ± 0.94* |
| PJ34-28 | 9 ± 0.82 |

D

**Johnsen Score Analysis (*$p < 0.05$)**

| | |
|---|---|
| Control PARP-1 NM | 9 ± 0.63 |
| DOX-7-PARP-1 NM | 8.6 ± 0.81 |
| DOX-28-PARP-1 NM | 6± 0.75* |
| Control PARP-1 KO | 8.83 ± 0.89 |
| DOX-7-PARP-1 KO | 7.5 ± 0.54* |
| DOX-28-PARP-1 KO | 5.66 ± 0.82* |

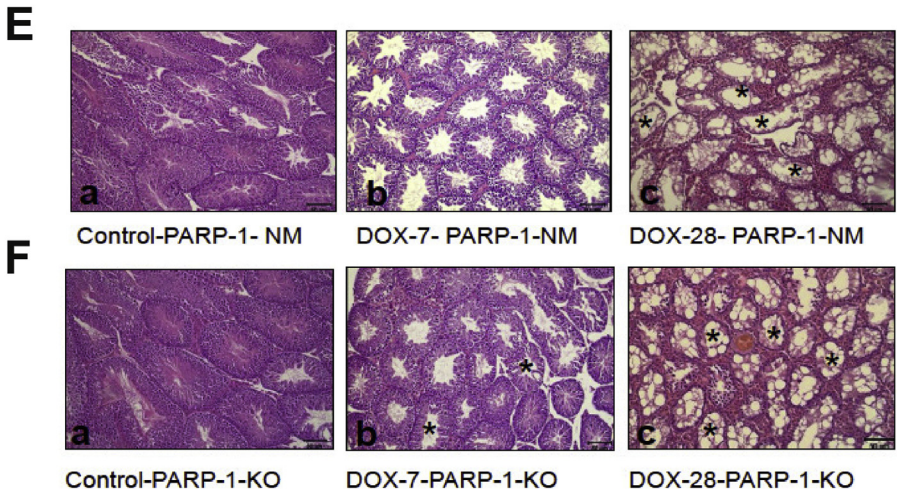


**Fig. 5.** Evaluation of testicular damage after 7 and 28 days following DOX-injection together with PJ34 treatment (A-C) and in PARP-1 knockout mice (D-F). (A) Control (a), DOX-7 (b), DOX+PJ34-7 (c), and PJ34-7 (d) groups had normal spermatogenesis with similar Johnsen scores (C) whereas in DOX-28 (b) group there was significant testicular damage with decreased Johnsen score (B and C). Testicular damage caused by DOX was prevented to some extent in DOX+PJ34-28 (c) group indicated by a better Johnsen score. (D-F) In PARP-1 NM testicular damage was present after 28 days of DOX-injection with a significant decrease in Johnsen score (D and E) whereas in PARP-1 KO mice DOX-injection caused significant testicular damage with decreased Johnsen scores both at 7 and 28 days indicating that if there is no PARP-1, testicular damage due to DOX is worsened (D and F). Scale bars: 50 μm.

mechanism of tissue damage in various pathological conditions related to oxidative stress [14,36,37]. After massive DNA damage, PARP plays a crucial role in cell death program by it's over activation. The excessive activation of PARP-1 in pathological conditions results in rapid depletion of intracellular $NAD^+$ [38,39]. In an attempt to restore the $NAD^+$ pools, NAD is resynthesized with a consumption of two to four molecules of ATP per molecule of $NAD^+$. This slows the rate of glycolysis and mitochondrial respiration, eventually leading to cellular dysfunction and death *via* apoptosis or necrosis.

**Table 1**
Mating rates and number of pups per litter after DOX-injection together with PJ34 treatment (n = 8).

| Groups | Mating (%) | Numbers of pups per litters (Mean ± SEM) |
|---|---|---|
| Control | 7/8 (%87.5) | 7.1 ± 0.8 |
| PJ34 | 7/8 (%87.5) | 7.5 ± 0.9 |
| DOX | **1/8 (%12.5)** | **4 ± 0*** |
| DOX + PJ34 | 3/8 (%37.5) | 7.3 ± 0.9 |

* $p < 0.05$.

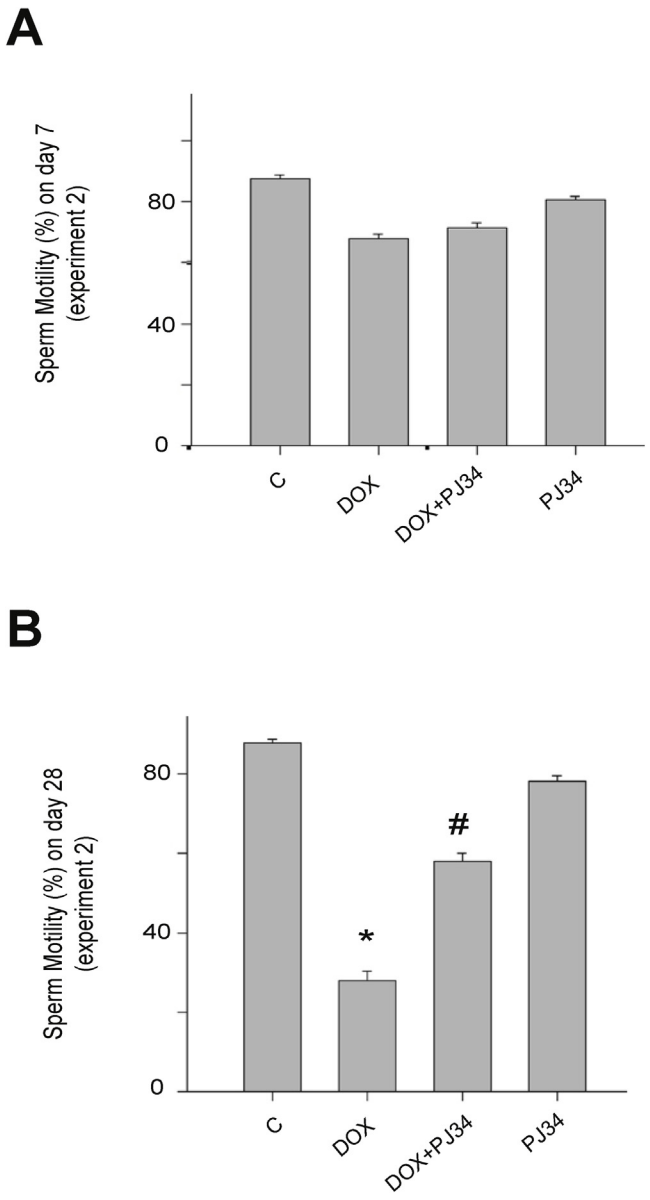


**Fig. 6.** Evaluation of sperm motility at 7 day (A) and 28 day (B) after DOX-administration. (B) Sperm motility decreased significantly at 28 day after DOX-injection. Administration of PJ34 together with DOX-injection significantly prevented it. $p<0.05$ for * and # in different pairwise comparisons.

To date, limited number of studies investigated the correlation between male infertility and PARP activation. A relationship between varicocele and PARP activation was shown previously, indicating increased cleaved-PARP1 expression in spermatogonia and spermatocytes in patients with varicocele [40]. Another study has revealed that over-activation of PARP-1 in rat testis by increased PARP-1 and PAR expressions were correlated with impaired testicular function related to varicocele [32]. Expression of PARP-1 protein was found to be higher in spermatocytes of old males when compared to the adolescent group [41] suggesting that DNA damage, which occurs concomitantly with increasing age, necessitates DNA repair and consequently results in high PARP levels. Our results demonstrated that DOX levels in plasma and testis tissues were high after administration of doxorubicin at 2 h and 4 h. Doxorubicin levels decreased after 7 days of DOX-injection however there was still some amount of DOX both in plasma and testis. Thus, possible effect(s) of DOX on male reproductive system could be explained by the possibility that DOX acted directly on the testes. There is evidence in the literature about the possible role of oxidative stress in the pathophysiology of DOX-induced cardiotoxicity [42]. We suggest that oxidative stress-triggered cellular events after DOX-injection resulting PARP-1 over-activation may contribute to the development of DOX-induced testicular damage and infertility in mice. Indeed, results of our study showed that cleaved PARP-1 and PAR expressions significantly increased within 2 h in testis following DOX-administration. This indicates the activation of PARP pathway within hours after DOX-injection.

PARP activation is robust in the DOX-induced rat testes producing variable lengths of PAR polymers as by-products of PARP activation. PAR has been linked to the p53 and caspases, which play an important role in apoptosis [43]. The results of the present study showed that PAR expression in testicular cells markedly increased after DOX administration, which may be responsible from apoptosis of cells in testes. Additionally, cleaved PARP and cleaved caspase-3 expression increased in DOX-treated group, which indicates cellular apoptosis in testes. Moreover, the results of the western blot findings confirmed that PARP inhibitor (PJ34) treatment together with DOX-administration resulted in a relatively small amount cleavage of PARP-1, and caspase-3 as well as decreased PAR formation. These results altogether demonstrated that inhibition of PARP over-activation by PJ34 treatment caused a significant reduction in apoptotic cell loss of testes caused by doxorubicin.

It has been reported that PARP-1 plays an important role in the caspase-dependent and caspase-independent apoptotic pathways following mitochondrial dysfunction. Caspase-dependent apoptosis is related to the activation of p53, which is a tumor suppressor protein. Chemotherapeutics can cause DNA damage and mitochondrial apoptosis by induction of p53, which is activated by the catalysis of PAR polymers after PARP activation [44]. It has been shown that DOX caused cardiotoxicity by inducing mitochondrial apoptosis through p53 [45]. Activation of the mitochondrial p53 pathway was also demonstrated in DOX-induced testicular germ cell loss [1]. According to our results we clearly showed that expression of both cleaved caspase-3 and p53 increased in testes after DOX-administration. It is known that PARP-1 is an important activator in caspase-independent cell death as well. PARP-1 regulates caspase-independent apoptotic signal transduction, whereby mitochondria release cytochrome c due to mitochondrial dysfunction [46]. Mitochondrial signaling pathway is also involved in germ cell apoptosis in the testes. Translocation of cytochrome c from mitochondria into cytosol is the primary event in mitochondrial signaling pathway for apoptosis [47]. Moreover, the release of cytochrome c from mitochondria is a primary site for Bcl-2 regulation of apoptosis [47]. The results of our study indicate that expression of caspase-independent apoptotic proteins, cytochrome c and AIF, increased significantly after DOX-administration. Taken together, these results suggest that both p53-mediated caspase-dependent mechanisms and caspase-independent mitochondrial signaling pathways may be regulated by PARP activation and are all involved in DOX-induced testicular apoptosis. In addition to analysis of proteins related with apoptotic cell loss, in the present study, successful induction of acute testicular toxicity

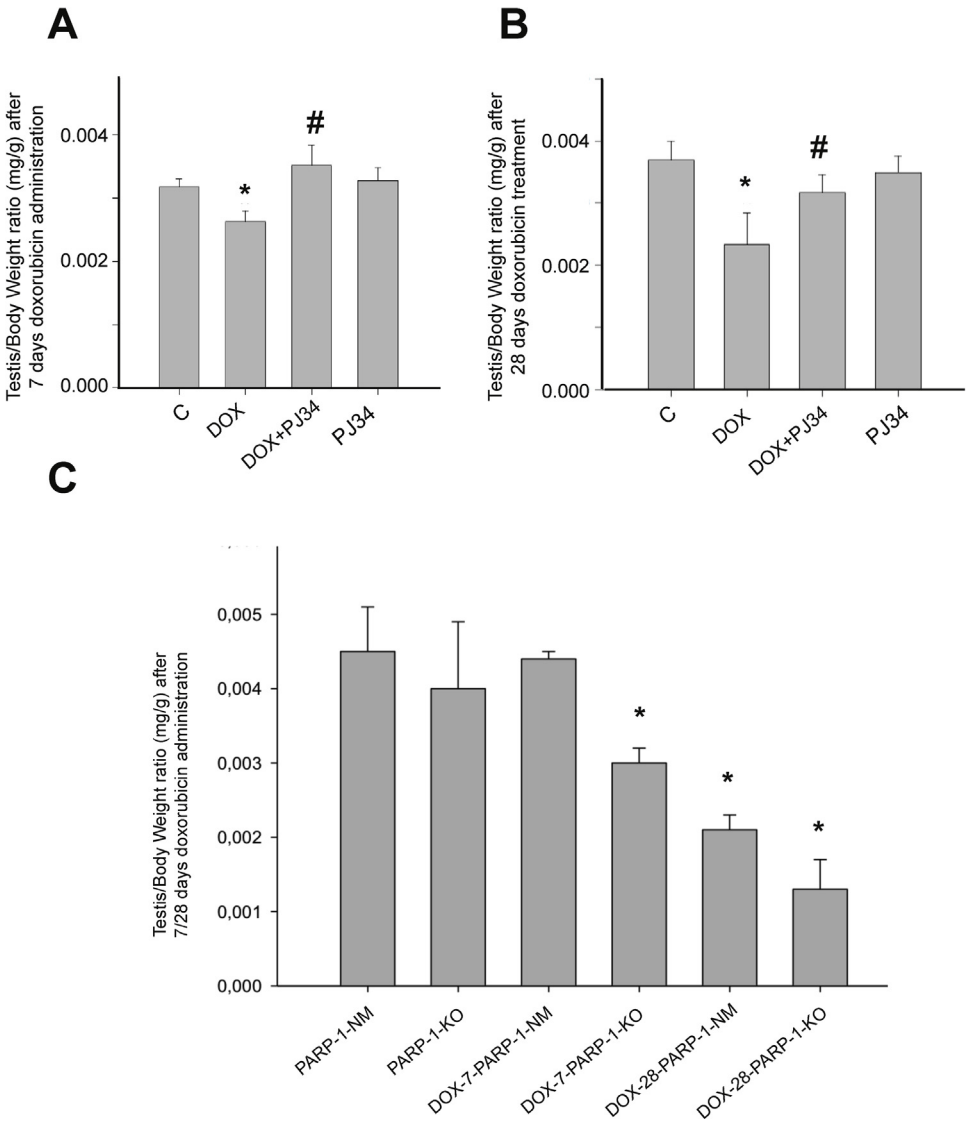


**Fig. 7.** Evaluation of testis and body weights after DOX-injection together with PJ34 treatment and in PARP-1 knockout mice. Testis weights decreased significantly in DOX group both at day 7 (A) and day 28 (B) after DOX-injection whereas PJ34 administration prevented this decrease both at day 7 and day 28 after DOX-injection. Testis weights of PARP-1 knockout mice decreased significantly in DOX-7-PARP-1-KO, DOX-28-PARP-1-NM, and DOX-28-PARP-1-KO groups (C). $p<0.05$ for * and # in different pairwise comparisons.

was confirmed also by histopathological evaluation after DOX-administration. Light microscopy and quantitative evaluation revealed testicular damage comprising various degrees of seminiferous tubule degeneration and germ cell loss after DOX-administration. Strikingly, PARP inhibitor treatment prevented testicular damage caused by DOX-injection by decreasing expression of PAR, p53, cleaved PARP-1, cleaved caspase-3, AIF, and cytochrome c levels.

Many clinical and experimental studies showed that toxic agents such as doxorubicin impairs male reproductive function by reducing semen quality, sperm concentration and motility [48,49]. Sperm motility is one of the important indirect parameters for fertilization that any negative effect on motility can change the fertilization capacity [50]. Thus, as shown in our results sperm motility decreases, starting from day 7 and persists until day 28 after DOX treatment. Our results suggest that after DOX-administration PARP activity increases and causes a significant decrease in sperm motility. This reduction in sperm motility can be associated with PARP over-activation, which may be related to ATP consumption. Besides sperm motility analyses we also showed that the number of pups per litters also decreased significantly after DOX-administration. Moreover, PARP inhibitor (PJ34) treatment together with DOX-administration prevented this decrease in sperm motility after 28 days.

On the other hand, we have found that when PARP-1 is totally absent in a knockout model, testes of mice treated with DOX show severe seminiferous tubule degeneration and germ cell loss was starting at first week after DOX-injection. Thus, our results suggested that removal of the PARP-1 gene might render testes more susceptible to cytotoxic agents, leading to more rapid and distinct cell loss [11]. The absence of PARP-1 may imply diminished capacity of DNA repair in germ cells and subsequent testicular damage. This was not the situation for PARP inhibition of DOX-induction where in that case PARP over-activity has been decreased to some extent but has not been removed totally.

In conclusion, our study indicates that PARP signaling pathway has an important role in DOX-induced testicular damage and fertility in mice. DOX-induced testicular damage is related to PARP-1 over-activation *via* both caspase-dependent and caspase-independent pathways. Inhibition of PARP over-activity efficiently

prevented testicular damage induced by doxorubicin by decreasing both mitochondria-dependent and -independent apoptotic pathways. Therefore, PARP inhibitors can be suggested as protective agents against DOX-induced testicular damage.

## Conflict of interest

None.

## Acknowledgments

Turkish Scientific and Research Council (TUBITAK) supported this work with project number of 110S377. This work was partially supported by the Akdeniz University Research Foundation, Antalya, Turkey.

## References

[1] Yeh YC, Lai HC, Ting CT, Lee WL, Wang LC, Wang KY, et al. Protection by doxycycline against doxorubicin-induced oxidative stress and apoptosis in mouse testes. Biochem Pharmacol 2007;74:969–80.
[2] Yeh YC, Liu TJ, Wang LC, Lee HW, Ting CT, Lee WL, et al. A standardized extract of Ginkgo biloba suppresses doxorubicin-induced oxidative stress and p53-mediated mitochondrial apoptosis in rat testes. Br J Pharmacol 2009;156:48–61.
[3] Tan C, Etcubanas E, Wollner N, Rosen G, Gilladoga A, Showel J, et al. Adriamycin–an antitumor antibiotic in the treatment of neoplastic diseases. Cancer 1973;32:9–17.
[4] Giri SN, Al-Bayati MA, Du X, Schelegle E, Mohr FC, Margolin SB. Amelioration of doxorubicin-induced cardiac and renal toxicity by pirfenidone in rats. Cancer Chemother Pharmacol 2004;53:141–50.
[5] Singal PK, Iliskovic N. Doxorubicin-induced cardiomyopathy. N Engl J Med 1998;339:900–5.
[6] Sreter I, Kiss A, Cornides A, Vereckei A, Toncsev H, Feher J. Inhibition of doxorubicin-induced liver toxicity by a new dihydroquinoline type antioxidant. Acta Physiol Hung 1984;64:431–5.
[7] Pacher P, Liaudet L, Bai P, Virag L, Mabley JG, Hasko G, et al. Activation of poly (ADP-ribose) polymerase contributes to development of doxorubicin-induced heart failure. J Pharmacol Exp Ther 2002;300:862–7.
[8] Pacher P, Liaudet L, Mabley J, Komjati K, Szabo C. Pharmacologic inhibition of poly (adenosine diphosphate-ribose) polymerase may represent a novel therapeutic approach in chronic heart failure. J Am Coll Cardiol 2002;40:1006–16.
[9] Szabo C. Poly (ADP-ribose) polymerase activation and circulatory shock. Novartis Found Symp 2007;280:92–103 discussion -7, 60-4.
[10] Winstall E, Affar EB, Shah R, Bourassa S, Scovassi IA, Poirier GG. Preferential perinuclear localization of poly(ADP-ribose) glycohydrolase. Exp Cell Res 1999;251:372–8.
[11] Xie Z, Zhou Y, Zhao W, Jiao H, Chen Y, Yang Y, et al. Identification of novel PARP-1 inhibitors: drug design, synthesis and biological evaluation. Bioorg Med Chem Lett 2015;25:4557–61.
[12] Burkart V, Wang ZQ, Radons J, Heller B, Herceg Z, Stingl L, et al. Mice lacking the poly (ADP-ribose) polymerase gene are resistant to pancreatic beta-cell destruction and diabetes development induced by streptozocin. Nat Med 1999;5:314–9.
[13] Szabo C, Cuzzocrea S, Zingarelli B, O'Connor M, Salzman AL. Endothelial dysfunction in a rat model of endotoxic shock. Importance of the activation of poly (ADP-ribose) synthetase by peroxynitrite. J Clin Invest 1997;100:723–35.
[14] Tasatargil A, Dalaklioglu S, Sadan G. Poly(ADP-ribose) polymerase inhibition prevents homocysteine-induced endothelial dysfunction in the isolated rat aorta. Pharmacology 2004;72:99–105.
[15] Thiemermann C, Bowes J, Myint FP, Vane JR. Inhibition of the activity of poly (ADP ribose) synthetase reduces ischemia-reperfusion injury in the heart and skeletal muscle. Proc Natl Acad Sci U S A 1997;94:679–83.
[16] Zingarelli B, Salzman AL, Szabo C. Genetic disruption of poly (ADP-ribose) synthetase inhibits the expression of P-selectin and intercellular adhesion molecule-1 in myocardial ischemia/reperfusion injury. Circ Res 1998;83:85–94.
[17] Qin WD, Liu GL, Wang J, Wang H, Zhang JN, Zhang F, et al. Poly(ADP-ribose) polymerase 1 inhibition protects cardiomyocytes from inflammation and apoptosis in diabetic cardiomyopathy. Oncotarget 2016;7:35618–31.
[18] Zhang R, Tang S, Huang W, Liu X, Li G, Chi H, et al. Protection of the brain following cerebral ischemia through the attenuation of PARP-1-induced neurovascular unit damage in rats. Brain Res 2015;1624:9–18.
[19] Leung M, Rosen D, Fields S, Cesano A, Budman DR. Poly(ADP-ribose) polymerase-1 inhibition: preclinical and clinical development of synthetic lethality. Mol Med. 2011;17:854–62.
[20] Pyriochou A, Olah G, Deitch EA, Szabo C, Papapetropoulos A. Inhibition of angiogenesis by the poly(ADP-ribose) polymerase inhibitor PJ-34. Int J Mol Med 2008;22:113–8.
[21] Kang J, Lee Y, No K, Jung E, Sung J, Kim Y, et al. Ginseng intestinal metabolite-I (GIM-I) reduces doxorubicin toxicity in the mouse testis. Reprod Toxicol 2002;16:291–8.
[22] Greene RF, Collins JM, Jenkins JF, Speyer JL, Myers CE. Plasma pharmacokinetics of adriamycin and adriamycinol: implications for the design of in vitro experiments and treatment protocols. Cancer Res 1983;43:3417–21.
[23] Speth PA, van Hoesel QG, Haanen C. Clinical pharmacokinetics of doxorubicin. Clin Pharmacokinet 1988;15:15–31.
[24] Robert J. Anthracyclines. In: Grochow Louise B, Ames Matthew M, editors. A Clinician's Guide to Chemotherapy Pharmacokinetics and Pharmacodynamics. The Williams & Wilkins Co.; 1998.
[25] Garcia Soriano F, Virag L, Jagtap P, Szabo E, Mabley JG, Liaudet L, et al. Diabetic endothelial dysfunction: the role of poly(ADP-ribose) polymerase activation. Nat Med 2001;7:108–13.
[26] Soriano FG, Pacher P, Mabley J, Liaudet L, Szabo C. Rapid reversal of the diabetic endothelial dysfunction by pharmacological inhibition of poly(ADP-ribose) polymerase. Circ Res 2001;89:684–91.
[27] Scott GS, Kean RB, Mikheeva T, Fabis MJ, Mabley JG, Szabo C, et al. The therapeutic effects of PJ34 [*N*-(6-oxo-5,6-dihydrophenanthridin-2-yl)-*N*,*N*-dimethylacetamide.HCl], a selective inhibitor of poly(ADP-ribose) polymerase, in experimental allergic encephalomyelitis are associated with immunomodulation. J Pharmacol Exp Ther 2004;310:1053–61.
[28] Suarez-Pinzon WL, Mabley JG, Power R, Szabo C, Rabinovitch A. Poly (ADP-ribose) polymerase inhibition prevents spontaneous and recurrent autoimmune diabetes in NOD mice by inducing apoptosis of islet-infiltrating leukocytes. Diabetes 2003;52:1683–8.
[29] Szabo C, Biser A, Benko R, Bottinger E, Susztak K. Poly(ADP-ribose) polymerase inhibitors ameliorate nephropathy of type 2 diabetic Leprdb/db mice. Diabetes 2006;55:3004–12.
[30] Koyun E, Okyay RE, Dogan OE, Kovali M, Dogan SS, Gulekli B. The effect of intrauterine insemination time on semen parameters. J Turk Ger Gynecol Assoc 2014;15:82–5.
[31] Celik-Ozenci C, Tasatargil A, Tekcan M, Sati L, Gungor E, Isbir M, et al. Effects of abamectin exposure on male fertility in rats: potential role of oxidative stress-mediated poly(ADP-ribose) polymerase (PARP) activation. Regul Toxicol Pharmacol 2011;61:310–7.
[32] Tekcan M, Koksal IT, Tasatargil A, Kutlu O, Gungor E, Celik-Ozenci C. Potential role of poly(ADP-ribose) polymerase activation in the pathogenesis of experimental left varicocele. J Androl 2012;33:122–32.
[33] Johnsen SG. Testicular biopsy score count—a method for registration of spermatogenesis in human testes: normal values and results in 335 hypogonadal males. Hormones 1970;1:2–25.
[34] Spina-Purrello V, Patti D, Giuffrida-Stella AM, Nicoletti VG. Parp and cell death or protection in rat primary astroglial cell cultures under LPS/IFNgamma induced proinflammatory conditions. Neurochem Res 2008;33:2583–92.
[35] Virag L, Szabo C. The therapeutic potential of poly(ADP-ribose) polymerase inhibitors. Pharmacol Rev 2002;54:375–429.
[36] Pacher P, Mabley JG, Soriano FG, Liaudet L, Komjati K, Szabo C. Endothelial dysfunction in aging animals: the role of poly(ADP-ribose) polymerase activation. Br J Pharmacol 2002;135:1347–50.
[37] Tasatargil A, Aksoy NH, Dalaklioglu S, Sadan G. Poly (ADP-ribose) polymerase as a potential target for the treatment of acute renal injury caused by lipopolysaccharide. Ren Fail 2008;30:115–20.
[38] Berger NA. Poly(ADP-ribose) in the cellular response to DNA damage. Radiat Res 1985;101:4–15.
[39] Schraufstatter IU, Hinshaw DB, Hyslop PA, Spragg RG, Cochrane CG. Oxidant injury of cells. DNA strand-breaks activate polyadenosine diphosphate-ribose polymerase and lead to depletion of nicotinamide adenine dinucleotide. J Clin Invest 1986;77:1312–20.
[40] El-Domyati MM, Al-Din AB, Barakat MT, El-Fakahany HM, Honig S, Xu J, et al. The expression and distribution of deoxyribonucleic acid repair and apoptosis markers in testicular germ cells of infertile varicocele patients resembles that of old fertile men. Fertil Steril 2010;93:795–801.
[41] El-Domyati MM, Al-Din AB, Barakat MT, El-Fakahany HM, Xu J, Sakkas D. Deoxyribonucleic acid repair and apoptosis in testicular germ cells of aging fertile men: the role of the poly(adenosine diphosphate-ribosyl)ation pathway. Fertil Steril 2009;91:2221–9.
[42] Cappetta D, De Angelis A, Sapio L, Prezioso L, Illiano M, Quaini F, et al. Oxidative stress and cellular response to doxorubicin: a common factor in the complex milieu of anthracycline cardiotoxicity. Oxid Med Cell Longev 2017;2017:1521020.
[43] Hong SJ, Dawson TM, Dawson VL. Nuclear and mitochondrial conversations in cell death: PARP-1 and AIF signaling. Trends Pharmacol Sci 2004;25:259–64.
[44] Mendoza-Alvarez H, Alvarez-Gonzalez R. Regulation of p53 sequence-specific DNA-binding by covalent poly(ADP-ribosyl)ation. J Biol Chem 2001;276:36425–30.
[45] Yoshida M, Shiojima I, Ikeda H, Komuro I. Chronic doxorubicin cardiotoxicity is mediated by oxidative DNA damage-ATM-p53-apoptosis pathway and attenuated by pitavastatin through the inhibition of Rac1 activity. J Mol Cell Cardiol 2009;47:698–705.
[46] Wu KL, Hsu C, Chan JY. Nitric oxide and superoxide anion differentially activate poly(ADP-ribose) polymerase-1 and Bax to induce nuclear translocation of apoptosis-inducing factor and mitochondrial release of cytochrome c after spinal cord injury. J Neurotrauma 2009;26:965–77.
[47] Kluck RM, Bossy-Wetzel E, Green DR, Newmeyer DD. The release of cytochrome c from mitochondria: a primary site for Bcl-2 regulation of apoptosis. Science 1997;275:1132–6.

[48] Ngoula F, Watcho P, Dongmo MC, Kenfack A, Kamtchouing P, Tchoumboue J. Effects of pirimiphos-methyl (an organophosphate insecticide) on the fertility of adult male rats. Afr Health Sci 2007;7:3–9.
[49] Mathur PP, D'Cruz SC. The effect of environmental contaminants on testicular function. Asian J Androl 2011;13:585–91.
[50] Hamilton JA, Cissen M, Brandes M, Smeenk JM, de Bruin JP, Kremer JA, et al. Total motile sperm count: a better indicator for the severity of male factor infertility than the WHO sperm classification system. Hum Reprod 2017; 2017:1521020.